Eurographics Workshop on Visual Computing for Biology and Medicine (2012)
T. Ropinski, A. Ynnerman, C. Botha, and J. B. T. M. Roerdink (Editors)

Combining B-Mode and Color Flow Vessel Segmentation for Registration of Hepatic CT and Ultrasound Volumes

Matthias Keil[1], Cristina Oyarzun Laura[1], Klaus Drechsler[1] and Stefan Wesarg[1]

[1]Department of Cognitive Computing & Medical Imaging, Fraunhofer IGD, Darmstadt, Germany, e-mail: matthias.keil@igd.fraunhofer.de

Abstract

Multimodal registration of intraoperative ultrasound and preoperative computed tomography imaging is the basis for percutaneous hepatic interventions. Currently, a rigid registration is performed manually by the surgeon using vessel structures and other anatomical landmarks for visual guidance. In this work our approach for intraoperative vessel segmentation from two ultrasound imaging modes, namely B-Mode and color flow mode, is presented. This segmentation is an important step for automation of the intraoperative registration which relies on vessel structures visible in contrast enhanced CT and ultrasound volumes. This paper describes the problems that arise when using B-mode ultrasound for segmentation of vessels and how they can be solved by introducing additional vessel information from color flow imaging. On a total number of 21 patients, our system was applied successfully in 15 cases. For nine randomly chosen patients studied in this paper, our system achieves a 3.45 mm accuracy at points used for registration and 5.01 mm for other landmarks which were not used for the registration process.

Categories and Subject Descriptors (according to ACM CCS): Image Processing and Computer Vision [I.4.6]: Segmentation—Image Processing and Computer Vision [I.4.m]: Miscellaneous—

1. Introduction

Orientation is a highly complex task in minimally invasive surgery. In order to know the location of the tools with respect to the target and risk structures, the surgeon needs a lot of experience.Ultrasound imaging is the modality of choice during percutaneous hepatic tumor ablations. The surgeon uses live ultrasound imaging at several stages of the workflow. Ultrasound B-Mode (BM) is used during diagnosis at the beginning of the intervention. Furthermore, it is used for orientation while searching for the tumor location and possible secondary findings. Finally, the interventional tool, which is most often a needle or cannula, is placed inside the tumor under ultrasound guidance.

During the intervention, the surgeon tries to enhance his understanding by overlapping preoperative contrast enhanced CT images with the intraoperative ultrasound [LVH*02]. This process is mainly performed mentally by the surgeon. The goal of the presented work is to extract vessel information from intraoperative imaging in order to enable an automatic registration of the imaging data. Even in open liver surgery the organ deformation usually stays in the range of 1-2 cm [HZB*10]. As the percutaneous ultrasound acquisition and the needle placement is performed under breath-hold, the deformation between the ultrasound image and the CT is expected to be much lower in our scenario. Therefore, a sufficiently good registration can be achieved by a rigid registration.

Despite the work in multimodal registration of ultrasound and CT, the alignment of the two volumes is still a complex and time consuming manual part of the the surgical intervention. After the ultrasound volume was acquired, the surgeon has to modify the translation and rotation parameters to generate a good matching which is evaluated based on the visual overlap of corresponding slices through the ultrasound and CT volume. In order to fulfill this task, the surgeon mainly uses vessel structures and bifurcations as internal landmarks. Our goal was to automate the time consuming manual registration process between preoperative CT and intraoperative BM ultrasound for percutaneous ablations.

We solved this problem by making use of the internal portal vein bifurcations as natural anatomical landmarks for an automatic rigid registration. This is similar to the surgeon's approach during manual registration. In order to build such a registration system, improvements were made in several key areas. First, we developed a robust and fast intraoperative BM and color flow vessel segmentation module. Another im-

DOI: 10.2312/VCBM/VCBM12/057-064

portant step was a new automatic graph based registration technique using the segmented vessel structures from CT and ultrasound volumes. This paper describes the problems arising in ultrasound vessel segmentation, demonstrates our approach for extracting more structures and presents the results of our rigid registration of pre- and intraoperative imaging data.

2. Previous Work

2.1. Vessel Segmentation

Although vessel segmentation is a very active topic in literature, only a few groups have been working on ultrasound data. The idea of height ridge traversal was presented by Aylward et al. [ABPE96]. It is based on the assumption that vessels are bright structures in a darker tissue. Using the Hessian matrix to calculate the second derivatives the centerline of this height ridge can be computed. Afterwards, a plane perpendicular to the vessel traverses this centerline in order to search for the vessel boundaries. Hassenpflug et al. [HSV*03] have shown the feasibility of vessel segmentation from two dimensional BM images based on simple thresholding. Lange et al. [LEH*04] described the use of vessels from Power Doppler ultrasound volumes without the need for vessel segmentation.

In opposition to the published results in ultrasound vessel segmentation, there are still some unresolved problems. Percutaneous ultrasound is most often acquired intercostal, where the transducer is placed between two ribs and rotated in a fan-like motion around the long axis of the piezoelectric crystal. The window through the ribs can be very small depending on the patient's anatomy. Due to partial reflection of the ultrasound signal caused by surfaces with high echogeneity or bad coupling of the transducer, large areas of the ultrasound BM volume contain hardly any vessel information (see Figure 1). This artifact is known as shadowing.

The proposed system overcomes this issue by acquiring color flow mode (CFM) data in addition to the BM images. Modern ultrasound machines allow for so called real-time duplex or triplex image acquisition. Using this technique, it is possible to acquire live BM and CFM images at the same time, as can be seen in Figure 1. The two resulting volumes after reconstruction are aligned and therefore information from both volumes can be used for vessel segmentation.

2.2. Vessel Based Registration

The group of Aylward et al. have made fundamental work in the field of vascular image registration. Their methods focus on the rigid alignment of vessel structure models to image data by evaluation of a registration metric. This metric is sampling the vessel centerlines and calculates the quality of the match based on the target image intensity at these locations proposing that the vessels are bright structures on a darker background [AJWB03].

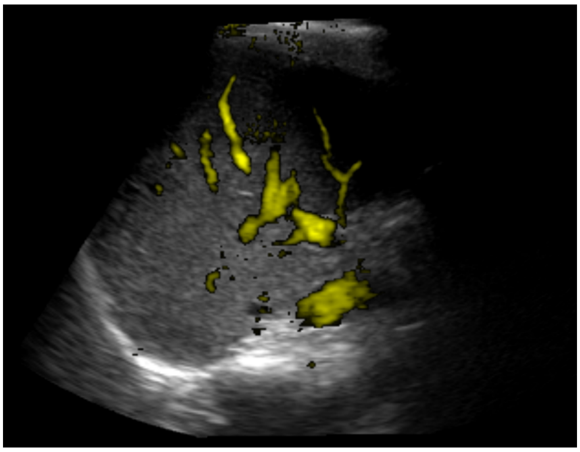

Figure 1: Shadowing artifact (upper right) in BM images caused by total reflection from the ribs. This image contains CFM data (yellow areas) overlaid on BM data.

Lange et al. presented in [LEH*04] a vessel based registration that uses the vessel bifurcations as landmarks for a rigid and deformable registration. The vessels are segmented from Power Doppler ultrasound images. Afterwards, the centerlines of the vessel structures are computed and used as landmarks for an adapted Iterative Closest Point (ICP) algorithm. The initialization of this registration is done by manual matching of four corresponding bifurcations in the intraoperative ultrasound centerlines and preoperatively created centerlines from CT imaging. The ICP algorithm then searches for additional point correspondences. As the closest centerline point from CT does not necessarily correspond to the same vessel in the ultrasound, the directions of the centerlines are considered.

3. Methodology

Our proposed registration system is based on the automatic matching of two segmented vessel graphs. Therefore, vessel segmentation from both preoperative CT and intraoperative ultrasound are important preprocessing steps. For better understanding, we are briefly describing our segmentation approach and the representation of the vessels as graphs. In order to calculate the transformation between the two vessel structures, we need to find the corresponding bifurcations which we use as landmarks for the rigid registration.

3.1. Intraoperative Ultrasound Imaging

The CT imaging and vessel tree segmentation are preoperative procedures which are not considered to be time critical. The segmentation is usually performed the day before the surgery or right before the patient arrives. Nevertheless, we are using a semi-automatic vessel segmentation technique requiring the definition of a single point inside the vessels [DOL10b]. Please note that this point can be everywhere inside the vessel tree of interest and does not have to be the root. The overall CT processing time is approximately 5-6 minutes. This does not include vessel tree separation, as this is not necessary for our task of registration with intraoperative ultrasound.

Ultrasound imaging and the necessary vessel segmentation are intraoperative steps. Therefore, they should be easy to perform and fast. Several different tracking methods for three dimensional ultrasound acquisition from two dimensional images have been presented in literature [SLT*07]. We are using the Virtual Navigator from Esaote S.p.A. and an electromagnetic tracking system to assemble the volume from images based on the position and orientation information. Such a freehand three dimensional percutaneous ultrasound scan can be performed either intercostal or subcostal. It usually takes less than 10 seconds and is part of the clinical routine of our partners. In fact, these scans are already repeated several times during the intervention. The segmentation should need as little input by the surgeon as possible. Our clinical partner asked for the overall run time for ultrasound segmentation and multimodal registration to stay below 3 minutes.

3.2. B-Mode Segmentation

The developed algorithm tries to segment the three dimensional lumen of the vessels, from which centerlines can be created. The input BM volume needs to be preprocessed in order to enhance the segmentation quality. A 3×3 median filter is applied to suppress noise.

The filtered BM volume is the input for the vesselness calculation. The proposed algorithm uses the multiscale vesselness computation method introduced by Sato et al. [SNA*97]. As in Sato's method the vesselness function is computed in the following way

$$f(\lambda_1, \lambda_c) = \begin{cases} e^{\frac{-\lambda_1^2}{2(\alpha_1 \lambda_c)^2}} & \lambda_1 \leq 0, \lambda_c \neq 0 \\ e^{\frac{-\lambda_1^2}{2(\alpha_2 \lambda_c)^2}} & \lambda_1 > 0, \lambda_c \neq 0 \\ 0 & \lambda_c = 0 \end{cases} \quad (1)$$

where $\alpha_1 = 0.5 < \alpha_2 = 2.0$ and $\lambda_c = \min(-\lambda_2, -\lambda_3)$.

This vesselness function is used to evaluate the eigenvalues $\lambda_1, \lambda_2, \lambda_3$ ($\lambda_1 > \lambda_2 > \lambda_3$) of the second order derivative, which is represented by the Hessian matrix, resulting in the response $R(x,y,z;\sigma)$ for each scale σ. The Hessian matrix was computed for $\sigma = \{1.0, 2.0, 3.0, 4.0\}$. The integration of the vessel response over the scales follows the adaptations from Drechsler et al. [DOL10b] and is called *Weighed Additive Response*. It can be written as

$$R(x,y,z) = \sum_{\sigma} \omega_\sigma \cdot R(x,y,z;\sigma). \quad (2)$$

The resulting vesselness information using $\omega_\sigma = 1$ is used as the input for a region growing based segmentation starting from a seed point placed inside the vessel lumen by the surgeon. As the vesselness response greatly depends on the vessel contrast in the original BM image, the user can adapt the region growing threshold with immediate feedback on the resulting segmentation.

In order to get a smoother representation of the vascular structure, the existing segmentation algorithm was extended by a level set thresholding using ITKs `ThresholdSegmentationLevelSetImageFilter`. The inputs to this filter are the segmented binary vessel image and the vesselness image. The same threshold that was used in the region growing step is applied during the level set filtering. As the level set result is not a binary image, a binarization is applied by labeling all voxels with values above a threshold $t > -1.5$ as vessels. The level set method does not only smooth the vessel boundaries, it can also overcome small gaps in the vesselness image. The main reason for these gaps are either inhomogeneities in the BM image, branches in the vascular tree, where the shape of the vessel differs from the assumed tubular shape, or low contrast between the vessel and the surrounding tissue. Please note that in BM only the wall of the portal vein reflects the ultrasound signal, and therefore results in a high contrast (cf. Figure 4a).

The BM segmentation algorithm works sufficiently good on images acquired percutaneously from healthy persons and patients who do not suffer from severe cirrhosis. In order to enhance the segmentation result for cirrhotic livers and volumes affected by artifacts, the segmentation of CFM data was implemented as described in the next subsection.

3.3. Color Segmentation

In order to achieve high quality CFM images the so called autocorrelation method is used for computation of the Doppler information on the ultrasound machine [LPG95]. Furthermore, the ultrasound machine keeps continuity over time and therefore smoothes the flow information of neighboring images in the volume along the sweep direction. Autocorrelation and continuity are used in order to overcome the limitations caused by shadowing and inhomogeneities. The CFM imaging is able to show structures even in areas where vessels are invisible in the BM image (cf. the upper right part Figure 1).

In our algorithm we assume the vessels to be symmetric tubular structures. The autocorrelation deforms the CFM information of a tubular vessel along the sweep direction, resulting in a drop-shaped structure (cf. the vessel profile on

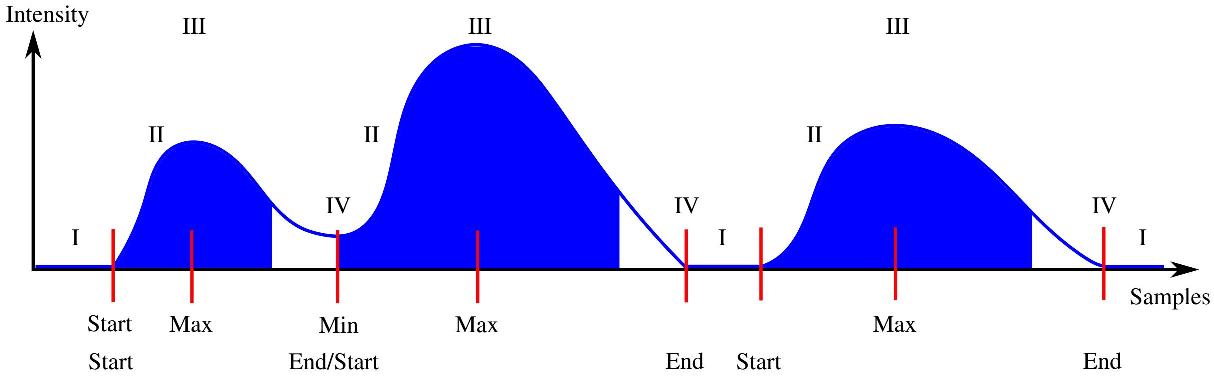

Figure 2: Schematic drawing of the CFM image processing algorithm. The curve in the diagram shows the image intensities sampled along the sweep direction through the volume. Outside of the vessels no CFM information was measured. Both autocorrelation and continuity stretch the vessel along the sweep direction. Therefore the vessel shape is distorted and neighboring vessels can be merged. The blue area represents the part of the vessel left after processing with the algorithm. The white area under the curve was removed from the vessel.

the right in Figure 2). Using the CFM information for segmentation would therefore lead to a dislocated vessel centerline. Another side effect of this smoothing is that locally distinct but neighboring vessels can be merged into a single CFM structure (cf. the two merged vessels on the left in Figure 2). Calculating the centerline of these vessels might result in additional branching points which are not existing in the real anatomy. Therefore, preprocessing of the CFM images is necessary before segmentation. At the beginning, a 5×5 median filter is applied to the CFM images in order to remove small artifacts and flashes, which can be caused by irregular transducer motion or the beating heart.

The next step is the sampling of the volume in order to find the vessel structures. The main sweep direction, which is approximately perpendicular to the ultrasound image plane, is known from the tracking information that was acquired for reconstruction of the ultrasound volume. A line-based sampling algorithm, which is looking for maxima along this sweep direction, was implemented. While proceeding along the line, the algorithm tests the current voxel value and keeps track of the detected vessels. Four stages, which can be seen in Figure 2, were defined describing the current situation at the sampling position:

I No vessel detected. No CFM information at current voxel. Proceed along sweep line.
II Voxel value > 0 detected. Vessel found. If in stage I or IV, remember current position as vessel starting point. If in stage II, keep track of vessel and count vessel voxels.
III Maximum along sweeping direction found. Continue search, remember number of vessel voxels on the line between starting point and maximum.
IV If in stage III and voxel value $= 0$ or local minimum found (neighboring CFM structures merged). End of vessel.

In order to reduce the effect of autocorrelation and continuity and therefore reshape the vessels to tubular structures, the additional CFM information needs to be removed. When the algorithm enters stage III it continues to sample along the line and tries to find a vessel end or a minimum. It then checks, whether the calculated number of voxels from start to maximum is less than the number of voxels from maximum to end (which is the case if the vessel was stretched). The difference in voxels will then be removed from the end of the vessel. This is shown in Figure 2 by the white areas preceeding the detected minimum or vessel ends.

As the algorithm works on single lines, postprocessing of the output becomes necessary in order to smooth the cropping of the vessels. The first step is a median filter, which removes small spikes on the vessel structures. Then a binarization of the image is performed in order to transform the CFM information into a binary segmentation result. Afterwards, a connected component analysis removes large artifacts like flashes from the vessel structures.

Besides the major advantages of CFM over BM images like high contrast, presence of almost only vascular structure, and structure even in areas of strong shadowing artifacts, there are also limitations. If a vessel runs perpendicular to the transducer plane, the CFM information disappears. Even with the use of pulsed Doppler, it might happen that no Doppler information can be measured in this situation and therefore no CFM can be calculated. In order to overcome this issue, a combined segmentation approach is presented in the next subsection.

3.4. Combined Segmentation

With combined segmentation the vascular structures from BM and CFM ultrasound are segmented. As both ultrasound volumes were acquired at the same time, they are perfectly

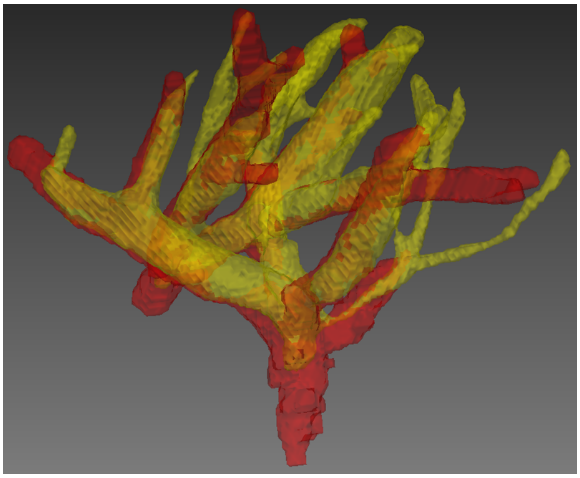

Figure 3: Surface visualization of the segmented vascular structure. The yellow part is the result of the CFM segmentation. The red part is the additional information from BM. Both structures combined represent the result of the combined method.

aligned. Therefore, the combined method was implemented as a union of the two binary volumes containing the segmented structures. An exemplary result of the combination can be seen in Figure 3.

The yellow structure represents the result of the CFM segmentation. This segmentation contains 11 bifurcation points, which can be used as landmarks, e.g. for a following registration process. Please note the thin vessels on the right, which were acquired inside a shadowing artifact as can be seen in Figure 1. The additional red part of this visualization was segmented from the BM volume. It also contains 11 bifurcation points. Please note that the bifurcation points of the two segmentations differ, as different vessels were visible in the datasets. Therefore, the combined method, which results in the complete tree, contains 16 bifurcations. Thus, using the combined method, the number of bifurcation points could be raised by 45% in this example.

The combined segmentation method combines the advantages of both ultrasound segmentation techniques described before. It overcomes the issue of perpendicular vessels, which can prevent the acquisition of color flow information. Furthermore, it contains vascular structure in areas affected by shadowing artifacts. As our registration is based on the vessel structures, the combined segmentation method increases the amount of information used for the alignment of pre- and intraoperative datasets.

3.5. Graph Matching and Registration

Due to limitations in both ultrasound volume size and quality, the segmented vessel structures contain loops and nearby vessels can be connected. Therefore, these structures can not be represented by trees. We chose a graph representation which is defined by nodes that represent vessel bifurcation points and edges which are representing the vessel centerlines. The graph properties further describe the vessel structures by including diameter, length, volume and angles between branches. For graph generation, we use the vessel centerlines extracted from the vessel segmenation result, as described in [DOL10a].

The resulting vessel graphs are matched using the algorithm described in [OLD11]. A thorough evaluation of this algorithm for ultrasound and CT matching can be found in [OLDE*12]. The graph matching approach has several advantages over an ICP matching which was decribed by Lange et al. [LEH*04]. At first, more information than just the direction of vessels is considered. Secondly, the graph matching results in an unambiguous assignment of correspondences between the bifurcations in the two datasets. Furthermore, the graph matching does not define wrong correspondences for a bifurcation if such a relationship can not be found adhering to the specifications defined in the algorithm. Last but not least, there is a chance for the ICP algorithm to get stuck in a local minimum resulting in a wrong registration.

With the one-to-one-correspondences given by the matching algorithm, we can calculate a rigid landmark transformation based on the bifurcation pairs. By calculating the Euclidean distances between the known point pairs, a registration can be calculated using the least squares method.

4. Results

4.1. Vessel Segmentation

We have evaluated the suitability of different vesselness measures for vessel segmentation from ultrasound. Figure 4 allows for a visual comparison between three of the most common vesselness measures. For all methods the standard parameter settings were used as described in the literature. The original B-Mode data is shown in Figure 4a. Figure 4b shows Sato's vesselness measure, which was used in the progress of this paper [SNA*97]. The result of Frangi's vesselness measure [FNVV98] can be seen in Figure 4c. The vesselness measure of Erdt et al. [ERS08] was used for enhancement in Figure 4d.

It can be seen that Frangi's method can lead to some continuity problems during the segmentation phase, as the vesselness measure falls off towards the vessel boundaries. For thinner vessels, the threshold based segmentation might stop at certain vessel locations especially at vessel bifurcations. Sato's and Erdt's method are visually almost identical. Comparing the vesselness values inside the vessels and in the surrounding parenchyma it can be seen that the contrast in Sato's method is slightly better, and therefore it was chosen for this work.

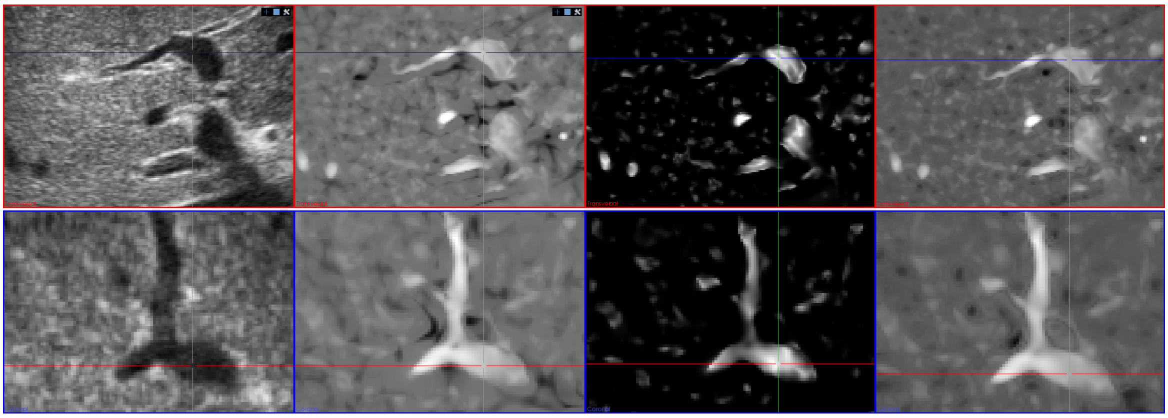

(a) B-Mode (b) Sato (c) Frangi (d) Erdt

Figure 4: Visual comparison of different vesselness measures for enhancement of ultrasound B-Mode vessels.

Table 1: Overview of the number of bifurcations segmented from corresponding BM and CFM volumes.

Dataset	# BM	# CFM	# Combined	Gain
1	14	14	23	64%
2	10	23	29	26%
3	4	23	27	17%
4	8	5	10	25%
5	4	14	18	28%
6	9	9	15	66%
7	13	9	16	23%
8	18	14	24	33%
9	10	16	20	25%

The presented algorithms for BM and CFM segmentation as well as the combined method are in regular clinical use. They serve as a preprocessing step for registration of intraoperative ultrasound and preoperative CT data. The usage of any of the algorithms depends mainly on the available data. Sometimes, only BM data is available and therefore the CFM and combined method can not be used. The methods were applied to ultrasound volumes of 47 patients. For 21 of those only BM volumes were acquired. For 25 patients both ultrasound volume types were available. In 5 cases the BM volumes did not contain any usable information and therefore only the CFM volumes could be segmented. The combination of the two imaging modes and the corresponding combined segmentation could be applied 9 times and on average the number of bifurcations was raised by 34% compared to segmenting BM and CFM separately, as can be seen in Table 1.

4.2. Vessel Based Registration

As mentioned above, the vessel structures inside the liver are considered as landmarks for the rigid registration process. As no ground truth registration was available, we are using a different approach for calculating the residual error in transformation. As was shown by Bauer et al. in [BPS*10] the vessel segmentation from contrast enhanced portal phase CT does have a high accuracy and shows a strong correspondence with the real vessel structures in the organ. Following this assumption and given a rigid registration as in our case, the residual registration error can be measured from the distances between the matched corresponding points in the CT and ultrasound datasets.

Table 2 gives an overview of the distance measures for 9 randomly chosen patients from our group of 27 patients for which we tried our registration system so far. Out of these 27 patients, in 6 cases the imaging quality of intraoperative Ultrasound or CT was compromised by imaging artifacts. In ultrasound imaging this can be insufficient coupling between the ultrasound transducer and the patient's body. One CT was impaired by a metallic stent in the vena cava resulting in large metal artifacts in the liver. Another possible cause for failure of vessel based registratioin was an unsufficient contrast agent distribution in the CT volume. From the remaining 21 patients the registration worked in 15 cases. In 6 cases the registration failed because the automatic matching did not find the correct matches.

A rigid registration with six degrees of freedom can not overcome position differences between the vessels caused by organ deformation between pre- and intraoperative imaging. Therefore, in the same dataset we can observe vessel bifurcations which are very close to each other after registration, as well as vessels that are not registered well. For example having a look at patient number 5 in Table 2, it can be seen that the minimum distance between corresponding bifurcations was 0.6 mm whereas the maximum observed distance is very high with 8.37 mm. The registration result of patient 5 can be seen in Figure 5.

Table 2: Distance measures for corresponding points inside the vessels. „Automatic" represents points chosen by the automatic graph matching. „Manual" represents points not used for the registration but for which reasonable correspondences could be established by manual inspection. „Time" gives the overall time necessary for intraoperative processing.

Patient	Automatic				Manual				
		Distances				Distances			
	Points	Min	Max	Mean	Points	Min	Max	Mean	Time
1	9	1.85	12.86	5.68	3	3.04	6.84	4.67	2:32
2	11	0.98	9.42	3.85	5	2.47	5.75	4.20	4:29
3	8	0.83	5.87	2.80	2	7.64	11.10	9.37	3:16
4	7	0.53	1.56	1.06	3	2.86	5.19	4.30	2:42
5	14	0.60	8.37	3.16	3	3.44	4.05	3.78	2:33
6	14	1.18	11.30	5.55	2	4.24	5.71	4.98	2:54
7	9	1.33	9.32	3.34	5	3.00	9.48	7.68	2:14
8	6	1.27	3.92	2.44	3	1.39	5.25	3.20	2:18
9	8	1.43	4.68	3.16	2	0.88	4.90	2.89	2:53
Average	9.6	1.11	7.48	3.45	3.1	3.22	6.48	5.01	2:52

Our landmark based registration algorithm considers all bifurcations as equally important for the registration process. Therefore, the mean distance between all landmarks measured over all patients is a good indication for the overall registration accuracy of the datasets. Our system achieves a 3.45 mm accuracy for the points used for registration and 5.01 mm for other landmarks which were not used for the registration process. It is noteworthy that the mean distances for the manually matched points is higher than that of the automatically matched points. This is based on the fact that these corresponding point pairs simply did not fulfill the criteria of the automatic matching algorithm, where distance between points is one criterion. Nevertheless, only plausible correspondences were matched manually. Therefore, the higher mean distances for these points are an indication of non-rigid deformation in the datasets.

Calculating the average values over all patients which were part of our study gives a good indication of two clinically important measures. First, the average registration accuracy of our algorithm, indicated by the mean distance values for automatically and manually matched points, as mentioned above. Second, the amount of deformation which can be expected in percutaneous procedures with different posture of the patients indicated by the maximum distances of the matched points. Here, we have observed an overall maximum deformation of approximately 13 mm.

The last column in Table 2 shows the overall time necessary for ultrasound vessel segmentation, post processing and volume registration. It can be seen that our algorithm usually stays within the 3 minute limit the clinical partner has defined.

5. Conclusions

We described our methodology to automate the intraoperative steps for multimodal registration, namely ultrasound vessel segmentation and rigid registration. To our knowledge, we are the first to address ultrasound vessel segmentation using both BM and CFM information. The registration based on graph matching has several advantages over other techniques presented in literature (e.g. ICP).

We presented two algorithms for segmentation of vascular structures from ultrasound volumes and a combination of both. The algorithms make use of the most common ultrasound imaging modes that are commonly used in the operating room: BM and CFM. The combined method overcomes the limitations of these two imaging modes. Therefore, the segmentations resulting from this combined method contain more branches and bifurcations.

Our system uses the bifurcations detected in preoperative CT and intraoperative ultrasound volumes as landmarks. We achieved a 3.45 mm accuracy for the points used for registration and 5.01 mm for other landmarks not used for the registration process. With a mean run time of under 3 minutes, our system is fast enough for intraoperative use. Based on a visual inspection of the registration results, an experienced surgeon acknowledged that our system is able to achieve better registration quality in a much shorter time than he could provide by manual registration.

Several improvements can be made in future development phases. First of all, the CFM segmentation could be extended by a deconvolution, defined by the point spread functions applied by autocorrelation and continuity. The combined method could be extended by a voting system, accounting for segmentation certainty of the two combined algorithms at a given location. Furthermore, a smoothing step applied to the data before vessel combination could overcome issues like location or diameter differences. Finally, the centerlines facilitate a search for possible vessel structures within a given neighborhood and along the principal axis of the vessels, enabling the algorithms to overcome small gaps in the calculated vesselness images or CFM data.

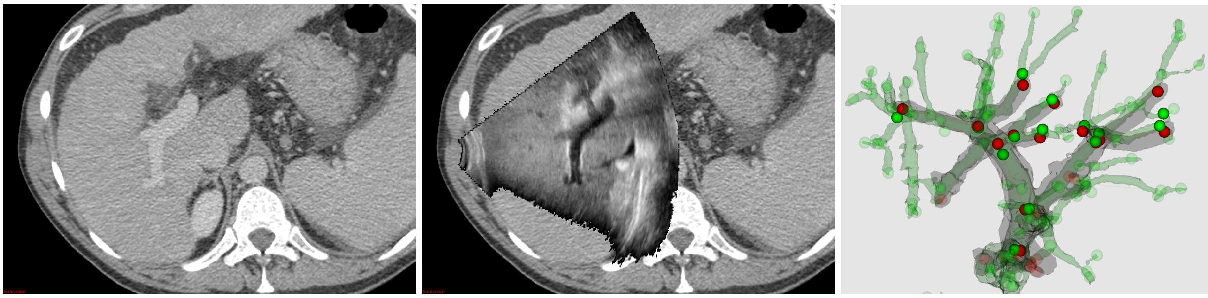

Figure 5: Registration result showing a transversal plane of the CT volume with the registered ultrasound and the vessel structures from CT (green) and ultrasound (red) with the automatically matched points highlighted.

Acknowlegment

The authors would like to thank Esaote S.p.A. for their support in ultrasound image acquisition and the Busto Arsizio General Hospital for their time and support in evaluation of the proposed method.

References

[ABPE96] Aylward S., Bullitt E., Pizer S., Eberly D.: Intensity ridge and widths for tubular object segmentation and description. In *Proceedings of the Workshop on Mathematical Methods in Biomedical Image Analysis, 1996.* (June 1996), pp. 131–138. 2

[AJWB03] Aylward S. R., Jomier J., Weeks S., Bullitt E.: Registration and analysis of vascular images. *International Journal of Computer Vision 55* (2003), 123–138. 2

[BPS*10] Bauer C., Pock T., Sorantin E., Bischof H., Beichel R.: Segmentation of interwoven 3d tubular tree structures utilizing shape priors and graph cuts. *Medical Image Analysis 14*, 2 (April 2010), 172–184. 6

[DOL10a] Drechsler K., Oyarzun Laura C.: Hierarchical decomposition of vessel skeletons for graph creation and feature extraction. In *IEEE International Conference on Bioinformatics and Biomedicine (BIBM), 2010* (December 2010), pp. 456–461. 5

[DOL10b] Drechsler K., Oyarzun Laura C.: A novel multiscale integration approach for vessel enhancement. In *Twenty-Third IEEE Symposium on Computer-Based Medical Systems 2010 - CBMS 2010* (2010), Dillon T. e. a., (Ed.), IEEE Computer Society Technical Committee on Computational Medicine, pp. 92–97. 3

[ERS08] Erdt M., Raspe M., Suehling M.: Automatic hepatic vessel segmentation using graphics hardware. In *Medical Imaging and Augmented Reality*, Dohi T., Sakuma I., Liao H., (Eds.), vol. 5128 of *Lecture Notes in Computer Science*. Springer Berlin / Heidelberg, 2008, pp. 403–412. 5

[FNVV98] Frangi A., Niessen W., Vincken K., Viergever M.: Multiscale vessel enhancement filtering. In *Medical Image Computing and Computer-Assisted Interventation - MICCAI 1998*, Wells W., Colchester A., Delp S., (Eds.), vol. 1496 of *Lecture Notes in Computer Science*. Springer Berlin / Heidelberg, 1998, pp. 130–137. 5

[HSV*03] Hassenpflug P., Schobinger M., Vetter M., Ludwig R., Wolf I., Thorn M., Grenacher L., Richter G. M., Uhl W., Buchler M. W., Meinzer H. P.: Generation of attributed relational vessel graphs from three-dimensional freehand ultrasound for intraoperative registration in image-guided liver surgery. *Proceedings of SPIE 5029* (May 2003), 222–230. 2

[HZB*10] Heizmann O., Zidowitz S., Bourquain H., Potthast S., Peitgen H.-O., Oertli D., Kettelhack C.: Assessment of intraoperative liver deformation during hepatic resection: Prospective clinical study. *World Journal of Surgery 34* (2010), 1887–1893. 1

[LEH*04] Lange T., Eulenstein S., Hünerbein M., Lamecker H., Schlag P.-M.: Augmenting intraoperative 3d ultrasound with preoperative models for navigation in liver surgery. In *Proceedings MICCAI 2004* (2004), pp. 534–541. 2, 5

[LPG95] Loupas T., Powers J., Gill R.: An axial velocity estimator for ultrasound blood flow imaging, based on a full evaluation of the doppler equation by means of a two-dimensional autocorrelation approach. *IEEE Transactions on Ultrasonics, Ferroelectrics and Frequency Control 42*, 4 (July 1995), 672–688. 3

[LVH*02] Lamadé W., Vetter M., Hassenpflug P., Thorn M., Meinzer H.-P., Herfarth C.: Navigation and image-guided hbp surgery: a review and preview. *Journal of Hepato-Biliary-Pancreatic Surgery 9* (April 2002), 592–599. 1

[OLD11] Oyarzun Laura C., Drechsler K.: Graph to graph matching: Facing clinical challenges. In *24th International Symposium on Computer-Based Medical Systems (CBMS), 2011* (June 2011), pp. 1–6. 5

[OLDE*12] Oyarzun Laura C., Drechsler K., Erdt M., Keil M., Noll M., De Beni S., Sakas G., Solbiati L.: Intraoperative registration for liver tumor ablation. In *Abdominal Imaging. Computational and Clinical Applications*, Yoshida H., Sakas G., Linguraru M., (Eds.), vol. 7029 of *Lecture Notes in Computer Science*. Springer Berlin / Heidelberg, 2012, pp. 133–140. 5

[SLT*07] Solberg O. V., Lindseth F., Torp H., Blake R. E., Nagelhus Hernes T. A.: Freehand 3d ultrasound reconstruction algorithms-a review. *Ultrasound in Medicine & Biology 33*, 7 (May 2007), 991–1009. 3

[SNA*97] Sato Y., Nakajima S., Atsumi H., Koller T., Gerig G., Yoshida S., Kikinis R.: 3d multi-scale line filter for segmentation and visualization of curvilinear structures in medical images. In *CVRMed-MRCAS'97*, Troccaz J., Grimson E., Mösges R., (Eds.), vol. 1205 of *Lecture Notes in Computer Science*. Springer Berlin / Heidelberg, 1997, pp. 213–222. 3, 5